



Published in final edited form as:

*Gastroenterology*. 2016 June ; 150(7): 1609–1619.e11. doi:10.1053/j.gastro.2016.02.025.

## Esophageal Expression of Active I $\kappa$ B kinase- $\beta$ in Mice Upregulates Tumor Necrosis Factor and Granulocyte Macrophage Colony-stimulating Factor, Promoting Inflammation and Angiogenesis

Marie-Pier Tétreault<sup>1,2,\*</sup>, Daniel Weinblatt<sup>1</sup>, Jody Dyan Ciolino<sup>3</sup>, Andres J Klein-Szanto<sup>4</sup>, Bridget K. Sackey<sup>1</sup>, Christina Twyman-Saint Victor<sup>1</sup>, Tatiana Karakasheva<sup>1</sup>, Valerie Teal<sup>5</sup>, and Jonathan P. Katz<sup>1</sup>

<sup>1</sup>Division of Gastroenterology, Department of Medicine, University of Pennsylvania Perelman School of Medicine, Philadelphia, PA, USA

<sup>2</sup>Department of Medicine, Gastroenterology and Hepatology Division, Northwestern University Feinberg School of Medicine, Chicago, IL, USA

<sup>3</sup>Department of Preventive Medicine, Feinberg School of Medicine, Northwestern University, Chicago, IL, USA.

<sup>4</sup>Department of Pathology, Fox Chase Cancer Center, Philadelphia, PA, USA

<sup>5</sup>Center for Clinical Epidemiology and Biostatistics, Department of Biostatistics and Epidemiology, University of Pennsylvania Perelman School of Medicine, Philadelphia, PA, USA

### Abstract

**Background & Aims**—I $\kappa$ B kinase- $\beta$  (IKK $\beta$ ) mediates activation of the nuclear factor- $\kappa$ B (NF $\kappa$ B), which regulates immune and inflammatory responses. Although NF $\kappa$ B is activated in cells from patients with inflammatory diseases or cancer, little is known about its roles in development and progression of esophageal diseases. We investigated whether mice that express an activated form of IKK $\beta$  in the esophageal epithelia develop esophageal disorders.

**Methods**—We generated *ED-L2-Cre/Rosa26-IKK2caSFL* mice, in which the ED-L2 promoter activates expression of Cre in the esophageal epithelia, leading to expression of a constitutively active form of IKK $\beta$  (IKK $\beta$ ca) in epithelial cells but not inflammatory cells or the surrounding stroma (IKK $\beta$ ca mice). Mice lacking the Cre transgene served as controls. Some mice were given intraperitoneal injections of neutralizing antibodies against granulocyte macrophage colony-

\*Correspondence: Marie-Pier Tétreault, Ph.D., Department of Medicine, Gastroenterology and Hepatology Division, Northwestern University Feinberg School of Medicine, 15-753 Tarry Building, 300 East Superior Street, Chicago, IL 60611-3010 USA; Tel.: 312-503-1915; Fax: 312-908-9032; marie-pier.tetreault@northwestern.edu.

**Publisher's Disclaimer:** This is a PDF file of an unedited manuscript that has been accepted for publication. As a service to our customers we are providing this early version of the manuscript. The manuscript will undergo copyediting, typesetting, and review of the resulting proof before it is published in its final citable form. Please note that during the production process errors may be discovered which could affect the content, and all legal disclaimers that apply to the journal pertain.

**Disclosures:** No conflicts of interest exist.

**Transcript Profiling:** Not applicable

stimulating factor (GMCSF) or tumor necrosis factor (TNF), or immunoglobulin G1 (control), starting at 1 month of age. Epithelial tissues were collected and analyzed by immunofluorescence, immunohistochemical, and quantitative real-time PCR assays. Transgenes were overexpressed from retroviral vectors in primary human keratinocytes.

**Results**—IKK $\beta$ ca mice developed esophagitis and had increased numbers of blood vessels in the esophageal stroma, compared with controls. Esophageal tissues from IKK $\beta$ ca mice had increased levels of GMCSF. Expression of IKK $\beta$ ca in primary human esophageal keratinocytes led to 11-fold overexpression of GMCSF and 200-fold overexpression of TNF. Incubation of human umbilical vein endothelial cells with conditioned media from these keratinocytes increased endothelial cell migration by 42% and promoted formation of capillary tubes; these effects were blocked by a neutralizing antibody against GMCSF. Injections of anti-GMCSF reduced angiogenesis and numbers of CD31+ blood vessels in esophageal tissues of IKK $\beta$ ca mice but did not alter the esophageal vasculature of control mice and did not alter recruitment of intraepithelial leukocytes to esophageal tissues of IKK $\beta$ ca mice. Injections of anti-TNF prevented development of esophagitis in IKK $\beta$ ca mice.

**Conclusions**—Constitutive activation of IKK $\beta$  in the esophageal epithelia of mice leads to inflammation and angiogenesis, mediated by TNF and GMCSF, respectively.

### Keywords

microenvironment; immune regulation; transcription factor; gene regulation

## Introduction

The mucosal integrity of the esophagus is regularly challenged by its continuous exposure to irritant factors such as refluxates of gastro-duodenal contents, alcohol, cigarette smoke, and hot beverages. Defective esophageal epithelial homeostasis has been linked to inflammation and injury and is implicated in the pathogenesis of esophageal diseases, resulting in significant morbidity, mortality, and health care expenditures<sup>1, 2</sup>. For example, esophageal cancer is the sixth most common cause of cancer-related death worldwide<sup>3</sup>, and most of these cancers arise from squamous mucosa<sup>4</sup>. Moreover, patients receiving irradiation for thoracic malignancies typically develop an acute esophagitis which can necessitate hospitalization or treatment interruption and eventually lead to stricture or ulceration<sup>5</sup>. Overall, a greater understanding of the mechanisms and consequences of esophageal inflammation and injury will lead to new therapeutic approaches for these diseases.

Dysregulation of signaling by the NF $\kappa$ B transcription factor family is associated with numerous inflammatory diseases and cancers, including reflux esophagitis<sup>6-10</sup>, and members of the NF $\kappa$ B family are pivotal for the maintenance of homeostasis by controlling diverse biological processes, such as inflammation, cell survival, and cell growth<sup>11</sup>. However, the direct consequences of NF $\kappa$ B activation on the esophageal microenvironment are not known, and the complex mechanisms by which NF $\kappa$ B signaling leads to the development and/or progression of esophageal diseases have yet to be determined.

The protein kinase IKK $\beta$  (IKK2), a member of the I $\kappa$ B kinase (IKK) complex, is responsible for activation of the NF $\kappa$ B signaling pathway<sup>12, 13</sup>. To date, most studies of epithelial IKK $\beta$  signaling have focused on processes intrinsic to epithelial cells, or linked to immune regulation. Yet epithelial inflammation has consequences outside of the epithelium, and our knowledge of the mechanisms by which epithelial IKK $\beta$  signaling modulates endothelial cells, immune cell recruitment, and other components of the stroma is still limited. Moreover, the effects of IKK $\beta$  activation on esophageal epithelial homeostasis have not been studied *in vivo*.

Here, we have utilized mice with activation of IKK $\beta$  specifically in the epithelia of the esophagus to demonstrate that epithelial IKK $\beta$  activation leads to esophagitis and to changes in the stromal vasculature. Moreover, epithelial IKK $\beta$  activation stimulates secretion of pro-angiogenic granulocyte-macrophage colony-stimulating factor (GM-CSF) by esophageal keratinocytes, resulting in neovascularization, and GM-CSF blockade prevents the pro-angiogenic effects of activated NF $\kappa$ B signaling *in vitro* and *in vivo*. Thus, epithelial IKK $\beta$  signaling is an important regulator of esophageal stromal vasculature through GM-CSF and of inflammation through TNF.

## Materials and Methods

### Generation of ED-L2-Cre/Rosa26-IKK2ca<sup>SFL</sup> Mice

All animal studies were approved by the Institutional Animal Care and Use Committee at the University of Pennsylvania. Mutant mice were hemizygous for Rosa26-Stop-Floxed-Constitutively active IKK2 (*Rosa26-IKK2ca<sup>SFL</sup>*, Jackson Laboratories, Bar Harbor, ME) and for the *Cre* transgene. All mice used for experiments were on a pure c57BL/6 background. For all experiments with *ED-L2-Cre/Rosa26-IKK2ca<sup>SFL</sup>* (*L2/IKK $\beta$ ca*) mice, sex-matched littermate *IKK2ca<sup>SFL</sup>* lacking the *Cre* transgene served as controls. Additional details are provided in the Supplementary Materials and Methods section.

### Cell Culture and Treatment

Mouse and primary human esophageal keratinocytes and primary human esophageal fibroblasts were isolated as described<sup>14</sup>. Human umbilical vein endothelial cells were purchased from Lonza (Walkersville, MD). Human Embryonic Kidney 293T cells, Phoenix-Ampho, and Phoenix-Eco cells were purchased from ATCC (Manassas, VA). Cells were cultured, transfected or infected, and quantitation was performed as described in the Supplementary Materials and Methods section.

### Immunofluorescence, Immunohistochemistry, and Microvessel density

Immunofluorescence and immunohistochemistry were performed using standard protocols. For descriptions of protocols and antibodies used, see the Supplementary Materials and Methods section. Blood vessels were visualized by staining endothelial cells with CD31 antibody. Six high-power fields were identified on each slide, and the MVDs were calculated as the total area of vessels in a  $\times 200$  field relative to the total stromal area.

### Western Blots

Western Blots were performed as described previously<sup>15</sup>. Additional details are provided in the Supplementary Materials and Methods section.

### RNA Analyses

RNA was extracted using the GeneJET RNA purification kit (Thermo Scientific, Pittsburg, PA) following the manufacturer's instructions. Quantitative real-time polymerase chain reaction (PCR) analyses were performed as described<sup>15</sup>. Additional details are provided in the Supplementary Materials and Methods section.

### Tube Formation Assay

Basement membrane extract (Trevigen, Gaithersburg, MD) was added to the wells of a 96-well plate and allowed to solidify at 37°C for 30 minutes. HUVEC (15,000 cells per well) were added in conditioned media from primary human esophageal keratinocytes, in the presence or absence of a neutralizing antibody against human GM-CSF (R&D systems). Cells were incubated at 37°C for 4h. The tubular networks were photographed in the wells using a Qimaging digital camera (Surrey, BC, Canada) attached to an inverted microscope (Leica DMIRB, Buffalo Grove, IL) with 10× objective.

### Endothelial Cell Migration Assay

HUVEC ( $5 \times 10^4$  cells) were added into the top chamber of an 8µM FluoroBlok insert (Corning) in 300µl of serum-free EBM2 media (Lonza) in triplicate. The inserts were placed into the bottom chamber of a 24-well plate containing conditioned media from primary human esophageal keratinocytes. At 24h, cells that migrated through the pores of the membrane to the bottom chamber were stained with calcein 8 µg/ml (Molecular Probes, Eugene, OR) in PBS for 30 min at 37°C. The fluorescence of migrated cells was quantified using a fluorescence microplate reader (Biotek FL×800, Winnoski, VT) at 485 nm excitation and 530 nm emission. Data are expressed as number of cells that migrated through or invaded pores +/- SEM.

### In vivo MP1-22E9 and XT3.11 treatment

Starting at 1 month of age, *L2/IKKβca* mice and littermate controls were given intraperitoneal injections of the GM-CSF neutralizing antibody MP1-22E9, the TNF neutralizing antibody XT3.11, IgG2a control (for MP1-22E9), or IgG1 control (for XT3.11) at doses of 800µg per mouse for MP1-22E9 or 500µg per mouse for XT3.11 (BioXCell, West Hanover, NH). Mice were treated every Monday and Thursday until they reached 1.5 month of age. The following numbers of matched littermate control and mutant mice were injected with neutralizing antibody or control: IgG2a, three pairs; MP1-22E9, three pairs. The following numbers of mutant mice were injected with neutralizing antibody or control: IgG1, four mice; and XT3.11, 4 mice.

### Statistical Analyses

Results were expressed as mean ± standard error of the mean, with statistical significance of differences between experimental conditions established at 95%. Two-way analysis of

variance (ANOVA) and Student *t* test were used to indicate the statistical difference between groups using GraphPad Prism version 4.0 (GraphPad Software, San Diego, CA). Additional details are provided in the Supplementary Materials and Methods section.

## Results

To delineate the role of epithelial NF $\kappa$ B/IKK $\beta$  signaling in the control of the esophageal microenvironment, we crossed *ED-L2/Cre* mice<sup>16</sup> to mice in which a constitutive active form of IKK $\beta$  (IKK $\beta$ ca) and EGFP were inserted into the endogenous ROSA26 locus (IKK2ca<sup>SFL</sup>; Jackson Laboratory)<sup>17</sup> (**Supplementary 1A**). *ED-L2/Cre* mice express Cre recombinase under the control of the Epstein-Barr Virus (EBV) *ED-L2* promoter, which drives transgenic expression specifically within the epithelia of the tongue, esophagus, and forestomach and the skin of the ventral neck<sup>15, 18</sup>. *L2/Cre;ROSA26-IKK $\beta$ ca+/L* mice (*L2/IKK $\beta$ ca* mice) had increased IKK $\beta$  signaling in esophageal epithelia, with increased IKK $\beta$  expression, and decreased expression of I $\kappa$ B $\alpha$ , a downstream target typically inhibited by IKK $\beta$  activation (**Supplementary Figure 1B**). Recombination efficiency within esophageal epithelia of 1 month-old *L2/IKK $\beta$ ca* mice was confirmed by immunofluorescence for EGFP (**Supplementary Figure 1D**). In contrast, no EGFP expression was observed in control mice (**Supplementary Figure 1C**).

At 1 month of age, *L2/IKK $\beta$ ca* mice demonstrated mild hyperplasia (**Figure 1B**), compared to littermate controls (**Figure 1A**). By 1.5 month of age, compared to control mice (**Figure 1C**), esophageal mucosa of *L2/IKK $\beta$ ca* mice became irregular, with the elongation of lamina propria papilla, and the presence of an inflammatory infiltrate (**Figure 1D**). By 3 months of age, the stromal architecture of *L2/IKK $\beta$ ca* mice was further disrupted (**Figure 1E**), compared to controls (**Figure 1E**), with hydropic changes, indicative of cellular injury (**Figure 1E, arrow**). BrdU labeling showed increased proliferation in esophageal epithelia of *L2/IKK $\beta$ ca* mice at 4 weeks of age (**Supplementary Figure 2A**). Interestingly, TUNEL assay revealed a dramatic increase in apoptotic cells of *L2/IKK $\beta$ ca* mice (**Supplementary Figure 2C**) compared to littermate controls (**Supplementary Figure 2B**) only at 3 months of age, suggesting a response of the epithelium to the inflammation seen at 6 weeks of age or a compensatory response to the increased proliferation. We also observed hyperplasia of the tongue and ventral neck skin but not the forestomach of *L2/IKK $\beta$ ca* mice (**Supplementary Figure 3**), and *L2/IKK $\beta$ ca* mice developed crusted skin lesions and alopecia that necessitated euthanasia by 3 months of age. No lesions were observed in control mice.

To confirm the presence of esophageal inflammation in *L2/IKK $\beta$ ca* mice, we stained esophageal mucosa of control and *L2/IKK $\beta$ ca* mice for the leukocyte marker CD45. Infiltrating leukocytes were observed in the epithelia and lamina propria of *L2/IKK $\beta$ ca* mice (**Figure 2B/D**), compared to controls (**Figure 2A/C**), at 6 weeks (**Figure 2A-B**) and 3 months (**Figure 2C-D**) of age. Using PCR arrays, we also observed statistically significant changes in expression of 13 cytokines, including several key chemokines, in esophageal epithelia isolated from 4 week-old *L2/IKK $\beta$ ca* mice, compared to epithelia from littermate controls (**Supplementary Table 1**). Among these, interleukin-10, lymphotoxin A, tumor necrosis factor, interleukin 12B, interleukin 12A, Chemokine (C-X-C motif) ligand 5,

granulocyte-macrophage stimulating factor, and thrombopoietin were upregulated in esophageal epithelia of *L2/IKKβca* mice, while bone morphogenetic protein 2, bone morphogenetic protein 7, macrophage migration inhibitory factor, bone morphogenetic protein 4, and cardiotrophin 1 were downregulated. To characterize the immune cell infiltrate observed in *L2/IKKβca* mice, we performed FACS analyses on spleen and esophagus from 6 week-old mice. We analyzed the leukocyte fraction (CD45+) for macrophages, natural killer cells (NK), dendritic cells (DC), myeloid-derived suppressor cells (MDSC), T-cells, T helper cells (Th), cytotoxic T cells (CTL), and regulatory T (Treg) cells (**Supplementary Table 2**). Among these, only MDSCs were significantly different between *L2/IKKβca* and control mice, when controlling for tissue type, with MDSCs increased by more 6-fold in esophageal epithelia and more than 9-fold in spleens of *L2/IKKβca* mice compared to controls. No significant changes were observed for macrophages, NK cells, DC, MDSC, T-cells, Th cells, CTL cells, and T-reg cells.

Initial histological studies of esophageal mucosa from *L2/IKKβca* mice suggested that these mice had alterations in their esophageal vasculature. To delineate the esophageal stromal vasculature of *L2/IKKβca* mice, we stained esophageal sections for the endothelial cell marker CD31 (**Figure 3A-B**). Compared to littermate controls, *L2/IKKβca* mice had a 3- to 4-fold increase in microvessel density (MVD) starting at 1.5 months of age (**Figure 3C**). Pericytes are mesenchymal-derived cells that support endothelial cell maturation and blood vessel integrity, and coverage of blood vessels by pericytes is reflective of a functional microvasculature<sup>19</sup>. By co-staining with CD31 for endothelial cells and desmin for pericytes (**Figure 3D-F**), we demonstrated that pericyte coverage was preserved in *L2/IKKβca* mice.

The formation of new vasculature shapes the microenvironment and has been detected early in the pre-malignant stages of cancer and in the context of inflammation and injury<sup>20</sup>. We hypothesized that pro-angiogenic factors were secreted by esophageal epithelial cells in response to IKKβ activation, leading to changes in the stromal vasculature. To identify these pro-angiogenic factors, we performed mouse cytokine/chemokine PCR arrays on esophageal epithelial peelings from *L2/IKKβca* mice at 1 month of age, before the onset of changes in the esophageal vasculature. Among the most highly induced pro-angiogenic factors was GM-CSF, which was increased by 4.6-fold in 1 month-old *L2/IKKβca* mice (**Figure 4A**). In contrast, expression of *VEGF*, a well-known inducer of angiogenesis, was not significantly changed (not shown). Immunohistochemistry also demonstrated increased GM-CSF in esophageal epithelia of 4 week-old *L2/IKKβca* mice (**Supplementary Figure 4B**) compared to littermate controls (**Supplementary Figure 4A**). To confirm that changes in *GM-CSF* mRNA expression were a direct effect of *IKKβ* activation, we infected primary human esophageal keratinocytes with *IKKβca* overexpressing retrovirus or control. Compared with control cells, *IKKβca* overexpressing primary human esophageal keratinocytes had an 11-fold induction in *GM-CSF* mRNA (**Figure 4B**). In addition, conditioned media from cultured primary human esophageal keratinocytes expressing *IKKβca* revealed increased secretion of GM-CSF, compared to controls (**Figure 4C**). Taken together, these data demonstrate that epithelial IKKβ promotes secretion of pro-angiogenic GM-CSF.

We next sought to determine whether increased angiogenesis with IKKβ activation was a direct result of GM-CSF secretion by esophageal epithelial cells. Treatment of HUVECs



with conditioned media from primary human esophageal keratinocytes expressing *IKKβca* increased capillary tube formation (**Figure 5C/E**), compared to controls (**Figure 5A/E**). This increase in tube formation was abolished by treatment with GM-CSF blocking antibody (**Figure 5D/E**). Importantly, GM-CSF neutralization did not affect tube formation when the assay was performed in the presence of conditioned media from keratinocytes expressing empty vector control (**Figure 5B/E**). We next performed endothelial cell migration assays in the presence of conditioned media from *IKKβca* expressing keratinocytes. HUVEC migration was increased by 42% in the presence of conditioned media from esophageal keratinocytes with constitutively active IKKβ, compared to controls, and GM-CSF neutralization blocked this increased cell migration (**Figure 5F**). GM-CSF blockade did not alter HUVEC cell migration treated with conditioned media from control esophageal keratinocytes (**Figure 5F**). Thus, increased epithelial IKKβ signaling promotes angiogenesis via GM-CSF.

To determine if GM-CSF was also responsible for neovascularization in mice with increased IKKβ signaling, we treated *L2/IKKβca* mice and littermate controls with the GM-CSF blocking antibody MP1-22E9 or IgG2a control. Control mice treated with IgG or MP1-22E9 had no differences in the esophageal vasculature or homeostasis (not shown). In contrast, compared to *L2/IKKβca* mice treated with IgG2a (**Figure 6A/D**), *L2/IKKβca* mice with GM-CSF neutralization (**Figure 6B/E**) had a significant reduction in the number of CD31+ blood vessels (**Figure 6C**) and VWF positive endothelial cells. GM-CSF can induce angiogenesis either by a direct effect on endothelial cells or through the recruitment of macrophages that subsequently release pro-angiogenic factors<sup>21-23</sup>. However, GM-CSF inhibition did not appear to alter recruitment of intraepithelial leukocytes, as we observed similar numbers of CD45+ cells in esophageal epithelia of *L2/IKKβca* mice treated with GM-CSF blocking antibody (**Supplementary Figure 5B**), compared to mutant mice treated with IgG2a control (**Supplementary Figure 5A**). Thus, IKKβ activation in keratinocytes induces GM-CSF secretion to triggers stromal neovascularization.

We next sought to determine whether other cytokines identified in our PCR array were responsible for the inflammatory response and immune cell infiltration in *L2/IKKβca* mice. Among the cytokines we identified as up-regulated in esophageal keratinocytes of mice with constitutively-active IKKβ was pro-inflammatory tumor necrosis factor (TNF), which was increased by 200-fold (**Supplementary Table 1**). Interestingly, TNF signaling drives accumulation of MDSCs<sup>24, 25</sup>, which were increased in *L2/IKKβca* mice. To determine if TNF was required for the inflammatory response and immune cell infiltration following IKKβ activation, we treated *L2/IKKβca* mice with the TNF neutralizing antibody XT3.11 or IgG1 control. *L2/IKKβca* mice treated with IgG1 had irregular basal layers (**Figure 7A**) compared to *L2/IKKβca* mice treated with XT3.11 (**Figure 7B**). Staining for the leukocyte marker CD45 showed decreased immune cell infiltration in the esophageal mucosa of *L2/IKKβca* mice treated with XT3.11 (**Figure 7D-E**) compared to *L2/IKKβca* mice treated with IgG1 (**Figure 7C/E**). Taken together, these data suggest that activation of epithelial IKKβ leads to inflammation and immune cell recruitment via TNF.

Inflammation is implicated in the development of numerous malignancies<sup>26-28</sup> including esophageal squamous cell cancer (ESCC), which often arises in the setting of chronic

inflammation<sup>15, 29-32</sup>. Yet the implications of activated IKK $\beta$ /NF $\kappa$ B signaling, GM-CSF upregulation, and increased TNF for human esophageal squamous cell carcinogenesis are not well defined. Using human tissue microarrays (TMA), we examined IKK $\beta$ /NF $\kappa$ B, GM-CSF, TNF, angiogenesis, and inflammation in normal and inflamed human esophageal tissues as well as human ESCC. Consistent with important functions during esophageal squamous cell carcinogenesis, p65 NF $\kappa$ B, GM-CSF, TNF, CD45, and microvessel density (MVD) all increased progressively from normal to inflamed human esophageal tissues and were highest in ESCC (Supplementary Figures 6-11 and Supplementary Tables 3-5). Moreover, in human ESCC, p65 NF $\kappa$ B expression correlated with expression of the IKK $\beta$ /NF $\kappa$ B targets GM-CSF and TNF (**Supplementary Table 6**), and TNF levels correlated with CD45 expression. However, none of these individual markers was significantly associated with the histopathological or clinical characteristics of the ESCC patients (**Supplementary Table 7**).

## Discussion

Esophageal homeostasis involves dynamic crosstalk between epithelial cells and underlying stromal cells. Yet, while alterations of the stromal microenvironment occur in esophageal diseases such as esophageal cancer and esophagitis, our knowledge of the molecular mechanisms that mediate changes in the microenvironment and that regulate epithelial-stromal interactions in the context of esophageal diseases is still very limited. Here, by activating IKK $\beta$ /NF $\kappa$ B signaling specifically in epithelial cells of the esophagus, we have interrogated the effects of epithelial inflammation on both esophageal epithelia and the stromal microenvironment. Moreover, this model has allowed us uniquely to define the consequences of esophageal inflammation in the early changes of esophageal diseases.

IKK $\beta$  activation in esophageal epithelia of mice causes esophagitis, with recruitment of intraepithelial leukocytes by 6 weeks of age and overt esophageal mucosal injury by 3 months of age. Interestingly, inflammation in *L2/IKK $\beta$ ca* mice develops in the absence of physical changes to increase acid or non-acid reflux. Moreover, this epithelial inflammation is sufficient to drive changes in not only the epithelia but also the surrounding stroma. Notably, increased levels of the pro-inflammatory cytokine TNF precede immune cell infiltration into the esophageal mucosa of *L2/IKK $\beta$ ca* mice, and TNF $\alpha$  blockade prevents immune cell accumulation in the esophageal mucosa following IKK $\beta$  activation. TNF signaling leads to accumulation of MDSCs<sup>24, 25</sup>, and MDSCs were increased by more than 6-fold in esophageal epithelia of *L2/IKK $\beta$ ca* mice. Since both TNF $\alpha$  and MDSCs are implicated in chronic inflammation and squamous cell carcinogenesis in mouse esophagus<sup>15, 29</sup>, we are currently investigating the role of TNF in MDSC recruitment following activation of epithelial IKK $\beta$ .

Our findings not only improve our understanding of the early stages of esophagitis but also provide important insights into the development of ESCC. IKK $\beta$ /NF $\kappa$ B signaling is elevated in patients with esophagitis, as well as those with esophageal squamous cell carcinoma<sup>33, 34</sup>. In fact, we demonstrated previously that the IKK $\beta$ /NF $\kappa$ B pathway is activated in a mouse that develops esophagitis and esophageal squamous cell carcinoma<sup>15</sup>. Moreover increased angiogenesis and GM-CSF expression are also observed in ESCC<sup>29, 35</sup>, and elevated levels



of GM-CSF correlate directly with future development of ESCC in high-risk patients<sup>36</sup>. Here, we demonstrate that p65 NF $\kappa$ B, GM-CSF, and TNF, along with angiogenesis and inflammation increase step-wise during progression from normal esophagus to esophageal inflammation to ESCC. An important caveat is no single factor among those that we examined predicts the histopathological or clinical characteristics of human ESCC, suggesting that other factors contribute to tumor growth, spread, and patient survival. Future studies will be directed towards determining the contributions of IKK $\beta$ /NF $\kappa$ B, GM-CSF, and TNF to human ESCC growth and progression and to identifying other key factors, ideally through a large clinical trial allowing the collection of both tissue and biochemical samples. Constitutive epithelial IKK $\beta$  activation induces spontaneous tumor formation and accelerates tumor initiation in the intestine<sup>37, 38</sup>. Unfortunately, because of a severe skin phenotype, *L2/IKK $\beta$ ca* mice cannot be aged beyond 3 months. Thus, to define the consequences of epithelial IKK $\beta$  activation on esophageal carcinogenesis, we are administering chemical carcinogens such as nitroso-compounds to *IKK $\beta$ ca* mice. Nonetheless, our current study provides compelling evidence for a role of the IKK $\beta$ /NF $\kappa$ B pathway and its downstream targets GM-CSF and TNF in the development of esophagitis and ESCC.

Angiogenesis is essential for tissue repair in inflammatory diseases and wound healing, and insufficient vascularization is associated with chronic, non-healing wounds<sup>39</sup>. However, angiogenesis must be tightly regulated, since uncontrolled neovascularization promotes the development and progression of cancer<sup>20</sup>. Our studies here demonstrate that constitutive activation of IKK $\beta$  in esophageal epithelial cells leads to GM-CSF production, resulting in increased neovascularization. GM-CSF can play a pro-angiogenic role either through the recruitment of macrophages or by acting directly on endothelial cells<sup>21-23</sup>. Since neovascularization precedes recruitment of intraepithelial leukocytes in the esophagus of *L2/IKK $\beta$ ca* mice, our data suggest that GM-CSF secretion directly activates esophageal neovascularization. However, given the functions of GM-CSF in myeloid cell differentiation<sup>40</sup>, we cannot exclude that GM-CSF also regulates angiogenesis indirectly through myeloid cells.

Recombinant GM-CSF promotes wound healing and angiogenesis in multiple tissues and contexts<sup>41-44</sup>. Of note, GM-CSF improves esophageal mucosal healing and enhances blood vessel formation in patients with severe radiation esophagitis<sup>45</sup>. However, human studies of radiation-induced esophagitis are challenging, due to difficulties with biopsying the region and attendant risks for the patient. Since whole-body irradiation models are well established in mice, molecular mechanisms of angiogenesis can readily be investigated in *L2/IKK $\beta$ ca* mice with radiation-induced esophageal injuries.

Another implication of our data is the potential dissociation of IKK $\beta$ /NF $\kappa$ B pathway effects in the esophagus on angiogenesis and on inflammation and immune cell recruitment. Theoretically, therapeutic strategies in esophageal diseases could be tailored towards either GM-CSF or TNF in order to specifically target angiogenesis or inflammation. In the future, we plan to delineate the consequences of modulating other cytokines that we have identified to be differentially expressed in *L2/IKK $\beta$ ca* mice compared to controls, allowing us to define the mechanisms underlying esophagitis and ESCC.

In sum, we propose a model (**Figure 7F**) in which IKK $\beta$  activation in esophageal epithelium promotes esophagitis and angiogenesis, triggering an epithelial-mesenchymal signaling network mediated by cytokine secretion from esophageal epithelial cells. We identify GM-CSF as an important pro-angiogenic factor secreted by esophageal keratinocytes following IKK $\beta$  activation that leads directly to stromal neovascularization. Furthermore, we identify TNF as a key pro-inflammatory cytokine necessary for inflammation and immune cell infiltration following IKK $\beta$  activation. As such, we define IKK $\beta$ , GM-CSF and TNF as potential therapeutic targets for esophagitis and ESCC.

## Supplementary Material

Refer to Web version on PubMed Central for supplementary material.

## Acknowledgments

**Grant Support:** This work was supported by: NIH NIDDK K99 DK094977, NIH NIDDK R00 DK094977, and a Zell Scholarship from the Robert H. Lurie Comprehensive Cancer Center to MPT; NIH NIDDK R01 DK069984 to JPK; the University of Pennsylvania Center for Molecular Studies in Digestive and Liver Diseases (NIH NIDDK P30 DK050306) through the Molecular Pathology and Imaging Core, the Molecular Biology/Gene Expression Core, the Cell Culture Core, and the Transgenic and Chimeric Mouse Core; NIH NCI P01 CA098101 (“Mechanisms of Esophageal Carcinogenesis”); and by the Robert H. Lurie Comprehensive Cancer Center (NIH NCI CCSG P30 CA060553) through the Northwestern University Mouse Histology and Phenotyping Core and the Northwestern University Center for Advanced Microscopy.

M.-P.T. designed and performed experiments, analyzed and interpreted data, obtained funding and wrote the manuscript; D.W. designed and performed experiments, analyzed and interpreted data; B.K.S. designed and performed experiments, analyzed and interpreted data; C.T-S. and T.K. designed and performed experiments, analyzed and interpreted data; V.L. and J.D.C. analyzed data; A.J.K-S. analyzed and interpreted data and J.P.K. designed experiments, analyzed and interpreted data, obtained funding, and wrote the manuscript.

## Abbreviations

<b>IKK<math>\beta</math></b>	IkappaB kinase beta
<b>GM-CSF</b>	Granulocyte Macrophage Colony-Stimulating Factor
<b>NF<math>\kappa</math>B</b>	Nuclear Factor Kappa B
<b>qPCR</b>	Quantitative real-time PCR
<b>TBP</b>	TATA box binding protein gene
<b>GAPDH</b>	Glyceraldehyde-3-phosphate dehydrogenase
<b>TNF</b>	Tumor necrosis factor
<b>ESCC</b>	Esophageal squamous cell cancer
<b>MVD</b>	Microvessel density

## References

1. Camilleri M, Dubois D, Coulie B, et al. Prevalence and socioeconomic impact of upper gastrointestinal disorders in the United States: results of the US Upper Gastrointestinal Study. *Clin Gastroenterol Hepatol.* 2005; 3:543–52. [PubMed: 15952096]

2. Shaheen NJ, Hansen RA, Morgan DR, et al. The burden of gastrointestinal and liver diseases, 2006. *Am J Gastroenterol*. 2006; 101:2128–38. [PubMed: 16848807]
3. Rustgi AK, El-Serag HB. Esophageal carcinoma. *N Engl J Med*. 2014; 371:2499–509. [PubMed: 25539106]
4. Jemal A, Center MM, DeSantis C, et al. Global patterns of cancer incidence and mortality rates and trends. *Cancer Epidemiol Biomarkers Prev*. 2010; 19:1893–907. [PubMed: 20647400]
5. Werner-Wasik M, Paulus R, Curran WJ Jr. et al. Acute esophagitis and late lung toxicity in concurrent chemoradiotherapy trials in patients with locally advanced non-small-cell lung cancer: analysis of the radiation therapy oncology group (RTOG) database. *Clin Lung Cancer*. 2011; 12:245–51. [PubMed: 21726824]
6. Yang J, Richmond A. Constitutive I $\kappa$ B kinase activity correlates with nuclear factor- $\kappa$ B activation in human melanoma cells. *Cancer Res*. 2001; 61:4901–9. [PubMed: 11406569]
7. Baldwin AS Jr. Series introduction: the transcription factor NF- $\kappa$ B and human disease. *J Clin Invest*. 2001; 107:3–6. [PubMed: 11134170]
8. Greten FR, Eckmann L, Greten TF, et al. IKK $\beta$  links inflammation and tumorigenesis in a mouse model of colitis-associated cancer. *Cell*. 2004; 118:285–96. [PubMed: 15294155]
9. Greten FR, Karin M. The IKK/NF- $\kappa$ B activation pathway—a target for prevention and treatment of cancer. *Cancer Lett*. 2004; 206:193–9. [PubMed: 15013524]
10. Vlantis K, Wullaert A, Sasaki Y, et al. Constitutive IKK2 activation in intestinal epithelial cells induces intestinal tumors in mice. *J Clin Invest*. 121:2781–93. [PubMed: 21701067]
11. Israel A. The IKK complex, a central regulator of NF- $\kappa$ B activation. *Cold Spring Harb Perspect Biol*. 2:a000158. [PubMed: 20300203]
12. Hacker H, Karin M. Regulation and function of IKK and IKK-related kinases. *Sci STKE*. 2006; 2006:re13. [PubMed: 17047224]
13. Huxford T, Huang DB, Malek S, et al. The crystal structure of the I $\kappa$ B $\alpha$ /NF- $\kappa$ B complex reveals mechanisms of NF- $\kappa$ B inactivation. *Cell*. 1998; 95:759–70. [PubMed: 9865694]
14. Yang Y, Goldstein BG, Nakagawa H, et al. Kruppel-like factor 5 activates MEK/ERK signaling via EGFR in primary squamous epithelial cells. *Faseb J*. 2007; 21:543–50. [PubMed: 17158781]
15. Tétreault MP, Wang ML, Yang Y, et al. Klf4 overexpression activates epithelial cytokines and inflammation-mediated esophageal squamous cell cancer in mice. *Gastroenterology*. 2010; 139:2124–2134. e9. [PubMed: 20816834]
16. Tétreault MP, Yang Y, Travis J, et al. Esophageal squamous cell dysplasia and delayed differentiation with deletion of kruppel-like factor 4 in murine esophagus. *Gastroenterology*. 2010; 139:171–81. e9. [PubMed: 20347813]
17. Sasaki Y, Derudder E, Hobeika E, et al. Canonical NF- $\kappa$ B activity, dispensable for B cell development, replaces BAFF-receptor signals and promotes B cell proliferation upon activation. *Immunity*. 2006; 24:729–39. [PubMed: 16782029]
18. Nakagawa H, Wang TC, Zukerberg L, et al. The targeting of the cyclin D1 oncogene by an Epstein-Barr virus promoter in transgenic mice causes dysplasia in the tongue, esophagus and forestomach. *Oncogene*. 1997; 14:1185–90. [PubMed: 9121767]
19. Murakami M, Simons M. Regulation of vascular integrity. *J Mol Med*. 2009; 87:571–82. [PubMed: 19337719]
20. Yoo SY, Kwon SM. Angiogenesis and its therapeutic opportunities. *Mediators Inflamm*. 2013; 2013:127170. [PubMed: 23983401]
21. Bussolino F, Ziche M, Wang JM, et al. In vitro and in vivo activation of endothelial cells by colony-stimulating factors. *J Clin Invest*. 1991; 87:986–95. [PubMed: 1705569]
22. Eubank TD, Roberts R, Galloway M, et al. GM-CSF induces expression of soluble VEGF receptor-1 from human monocytes and inhibits angiogenesis in mice. *Immunity*. 2004; 21:831–42. [PubMed: 15589171]
23. Roda JM, Sumner LA, Evans R, et al. Hypoxia-inducible factor-2 $\alpha$  regulates GM-CSF-derived soluble vascular endothelial growth factor receptor 1 production from macrophages and inhibits tumor growth and angiogenesis. *J Immunol*. 2011; 187:1970–6. [PubMed: 21765015]

24. Hu X, Li B, Li X, et al. Transmembrane TNF- $\alpha$  promotes suppressive activities of myeloid-derived suppressor cells via TNFR2. *J Immunol.* 2014; 192:1320–31. [PubMed: 24379122]
25. Zhao X, Rong L, Zhao X, et al. TNF signaling drives myeloid-derived suppressor cell accumulation. *J Clin Invest.* 2012; 122:4094–104. [PubMed: 23064360]
26. Coussens LM, Werb Z. Inflammation and cancer. *Nature.* 2002; 420:860–7. [PubMed: 12490959]
27. Grivennikov SI, Greten FR, Karin M. Immunity, Inflammation, and Cancer. *Cell.* 2010; 140:883–899. [PubMed: 20303878]
28. Hanahan D, Weinberg Robert A. Hallmarks of Cancer: The Next Generation. *Cell.* 144:646–674. [PubMed: 21376230]
29. Stairs DB, Bayne LJ, Rhoades B, et al. Deletion of p120-catenin results in a tumor microenvironment with inflammation and cancer that establishes it as a tumor suppressor gene. *Cancer Cell.* 2011; 19:470–83. [PubMed: 21481789]
30. Ribeiro U Jr, Posner MC, Safatle-Ribeiro AV, et al. Risk factors for squamous cell carcinoma of the oesophagus. *Br J Surg.* 1996; 83:1174–85. [PubMed: 8983603]
31. Liu K, Jiang M, Lu Y, et al. Sox2 cooperates with inflammation-mediated Stat3 activation in the malignant transformation of foregut basal progenitor cells. *Cell Stem Cell.* 2013; 12:304–15. [PubMed: 23472872]
32. Diakowska D. Cytokines association with clinical and pathological changes in esophageal squamous cell carcinoma. *Dis Markers.* 2013; 35:883–93. [PubMed: 24427776]
33. Li B, Li YY, Tsao SW, et al. Targeting NF- $\kappa$ B signaling pathway suppresses tumor growth, angiogenesis, and metastasis of human esophageal cancer. *Mol Cancer Ther.* 2009; 8:2635–44. [PubMed: 19723887]
34. O'Riordan JM, Abdel-latif MM, Ravi N, et al. Proinflammatory cytokine and nuclear factor kappa-B expression along the inflammation-metaplasia-dysplasiaadenocarcinoma sequence in the esophagus. *Am J Gastroenterol.* 2005; 100:1257–64. [PubMed: 15929754]
35. Liu J, Li Z, Cui J, et al. Cellular changes in the tumor microenvironment of human esophageal squamous cell carcinomas. *Tumour Biol.* 2012; 33:495–505. [PubMed: 22134872]
36. Keeley BR, Islami F, Pourshams A, et al. Prediagnostic serum levels of inflammatory biomarkers are correlated with future development of lung and esophageal cancer. *Cancer Sci.* 2014; 105:1205–11. [PubMed: 25040886]
37. Vlantis K, Wullaert A, Sasaki Y, et al. Constitutive IKK2 activation in intestinal epithelial cells induces intestinal tumors in mice. *J Clin Invest.* 2011; 121:2781–93. [PubMed: 21701067]
38. Shaked H, Hofseth LJ, Chumanevich A, et al. Chronic epithelial NF- $\kappa$ B activation accelerates APC loss and intestinal tumor initiation through iNOS up-regulation. *Proc Natl Acad Sci U S A.* 2012; 109:14007–12. [PubMed: 22893683]
39. Adams RH, Alitalo K. Molecular regulation of angiogenesis and lymphangiogenesis. *Nat Rev Mol Cell Biol.* 2007; 8:464–78. [PubMed: 17522591]
40. Hamilton JA, Achuthan A. Colony stimulating factors and myeloid cell biology in health and disease. *Trends Immunol.* 2013; 34:81–9. [PubMed: 23000011]
41. Fang Y, Shen J, Yao M, et al. Granulocyte-macrophage colony-stimulating factor enhances wound healing in diabetes via upregulation of proinflammatory cytokines. *Br J Dermatol.* 2010; 162:478–86. [PubMed: 19799605]
42. Gulcelik MA, Dinc S, Dinc M, et al. Local granulocyte-macrophage colony-stimulating factor improves incisional wound healing in adriamycin-treated rats. *Surg Today.* 2006; 36:47–51. [PubMed: 16378193]
43. Ergun SS, Kyran B, Su O, et al. Effects of granulocyte macrophage colony stimulating factor on random flap healing and immune profile in rats with impaired wound healing by glucocorticoids. *Ann Plast Surg.* 2004; 52:80–8. [PubMed: 14676705]
44. Memisoglu E, Oner F, Ayhan A, et al. In vivo evaluation for rhGM-CSF wound-healing efficacy in topical vehicles. *Pharm Dev Technol.* 1997; 2:171–80. [PubMed: 9552443]
45. Koukourakis MI, Flordellis CS, Giatromanolaki A, et al. Oral administration of recombinant human granulocyte macrophage colony-stimulating factor in the management of radiotherapy-induced esophagitis. *Clin Cancer Res.* 1999; 5:3970–6. [PubMed: 10632327]

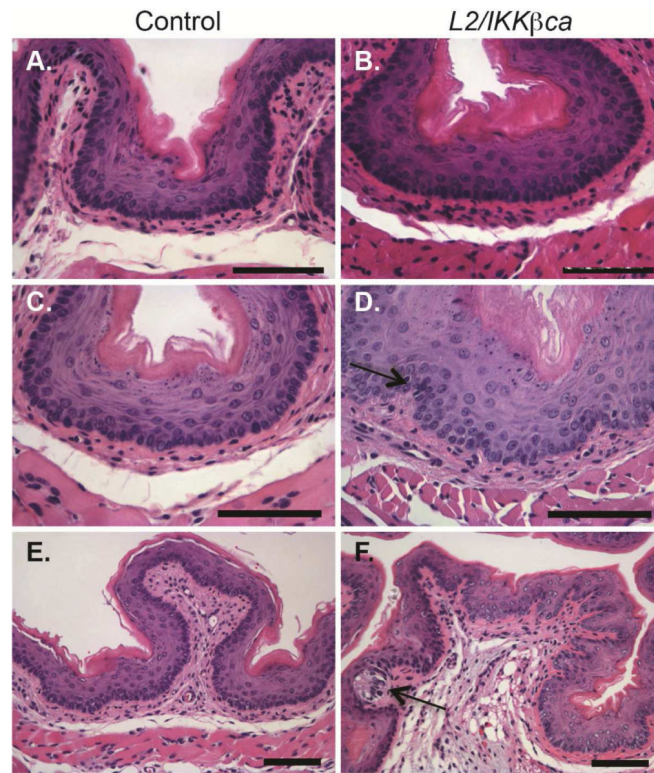


**Figure 1.** Epithelial specific IKK $\beta$  activation alters the esophageal microenvironment. (A-B) At 1 month of age, mice with increased epithelial IKK $\beta$  signaling had epithelial hyperplasia (B), compared to littermate controls (A). (n=5 mice per group) (C-D) At 1.5 month of age, control mice (C) demonstrated homogenous basal cells while basal layers of *L2/IKK $\beta$ ca* mice (D) were expanded and irregular. Moderate inflammatory infiltrates were also observed (arrow). (n=8 mice per group) (E-F). At 3 months of age, hydropic changes (arrow) and stromal remodeling were seen in the esophageal microenvironment of *L2/IKK $\beta$ ca* mice (F), compared to controls (E). (n=5 mice per group) Scale bars, 25  $\mu$ m.



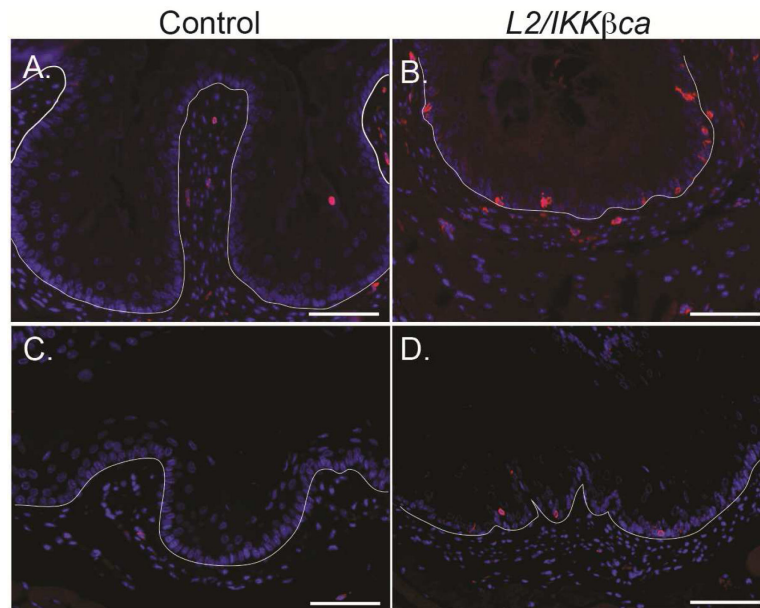


**Figure 2.** *L2/IKKβca* mice have increased esophageal infiltration of immune cells. (A-D) Esophageal mucosa of control mice (A/C) contained few leukocytes, as indicated by staining for CD45, but multiple leukocytes were present in esophageal epithelia and lamina propria of *L2/IKKβca* mice (B/D) at 6 weeks of age (A-B) (n=8 mice per group) and 3 months of age (C-D) (n=5 mice per group). Scale bars: 25μm.



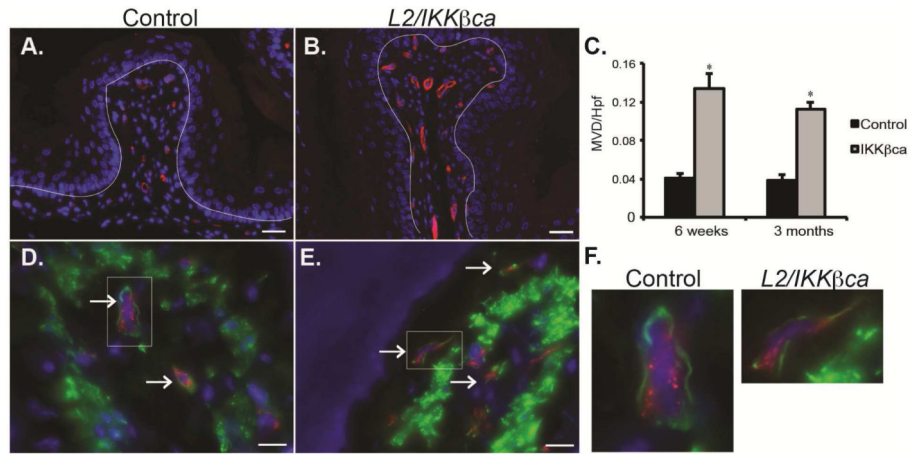


**Figure 3.**

*L2/IKKβca* mice have increased angiogenesis. (A-B) At 1.5 months of age, *L2-IKKβca* mice (B) had increased staining for the endothelial cell marker CD31 (red) compared to littermate controls (A). DAPI was used as a nuclear stain, and the dotted line was drawn to demonstrate the location of the basement membrane. (n=8 mice per group) Scale bars, 25  $\mu$ m. (C) Quantification of microvessel density per high power field (MVD/hpf) revealed a statistically significant (\* $p < 0.05$ , Student *t* test) increase in *L2/IKKβca* mice beginning at 1.5 months of age. (D-E) Co-staining for the endothelial cell marker CD31 (red) and the smooth muscle cell marker desmin (green) revealed no difference in pericyte coverage between 6 week-old control (D) and *L2/IKKβca* mice (E). (F) Left panel: Insert from picture in 3D, Right panel: Insert from picture in 3E. (n=4 mice per group).

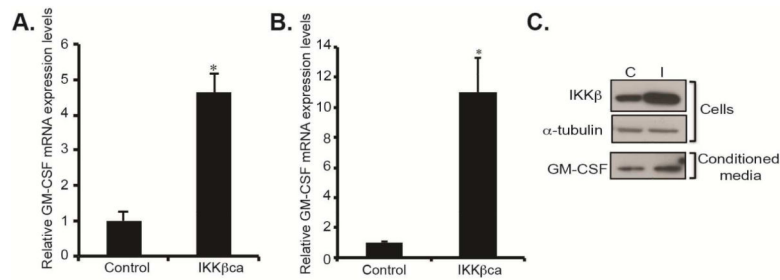


**Figure 4.**

Activation of epithelial IKK $\beta$  signaling leads to increased GM-CSF expression and secretion. **(A)** By quantitative real-time PCR, *GM-CSF* mRNA expression levels were induced 4.6-fold in esophageal epithelia of 4 week-old *L2/IKK $\beta$ ca* mice (n=3). \*Significant difference from control at p-value of less than 0.01. **(B)** In immortalized primary human esophageal keratinocytes retrovirally transduced to express constitutively-active IKK $\beta$ , *GM-CSF* mRNA expression was increased by 11-fold, compared with esophageal keratinocytes with control plasmid (n=4). \* Significant difference from control plasmid at p-value of less than 0.01, Student *t* test. **(C)** Primary human esophageal keratinocytes with increased IKK $\beta$  signaling had increased secretion of GM-CSF in their conditioned media, compared to control cells (n=4).

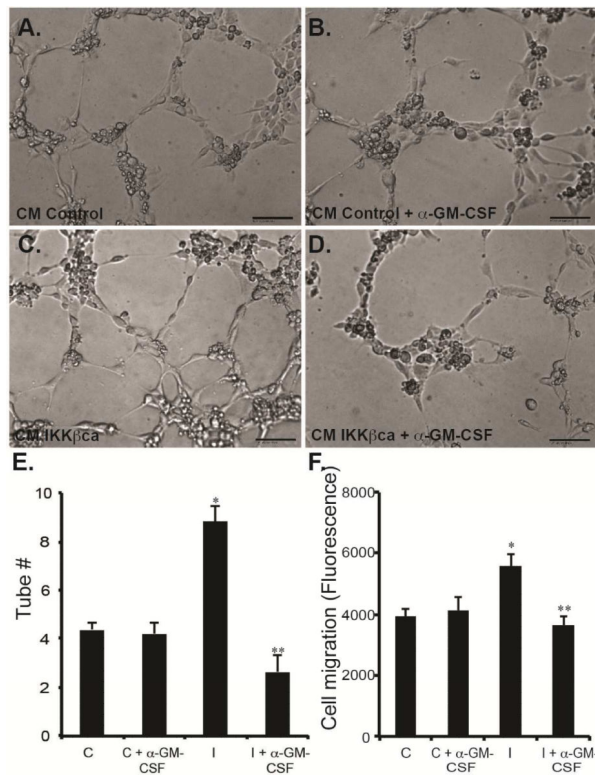


**Figure 5.** Epithelial-derived GM-CSF promotes angiogenesis *in vitro*. (A-D) In a tube formation assay, HUVEC cultured in the presence of conditioned media from human esophageal keratinocytes with constitutively-active IKK $\beta$  had increased ability to form tubes (C), compared to HUVEC treated with conditioned media from control esophageal keratinocytes (A). (B/D) Treatment with a blocking antibody against GM-CSF abolished the increased tube formation induced by the presence of conditioned media from esophageal keratinocytes with increased IKK $\beta$  signaling (D) but did not affect control cells (B). (n=3 in triplicates) (E) Quantification of the number of tubes per high power field in cells treated with control (C) and IKK $\beta$ ca (I) conditioned media, with and without GM-CSF blockade. (F) Transwell assays demonstrated that conditioned media from esophageal keratinocytes with constitutively-active IKK $\beta$  increased HUVEC cell migration, compared to control cells. GM-CSF blockade abolished the increased cell migration of HUVEC incubated in the presence of conditioned media from esophageal keratinocytes with active IKK $\beta$ . (n=3 in triplicates) \*Significant difference from control plasmid at p-value of less than 0.01. \*\* Significant difference from IKK $\beta$ ca at p-value of less than 0.01, Student *t* test and ANOVA.

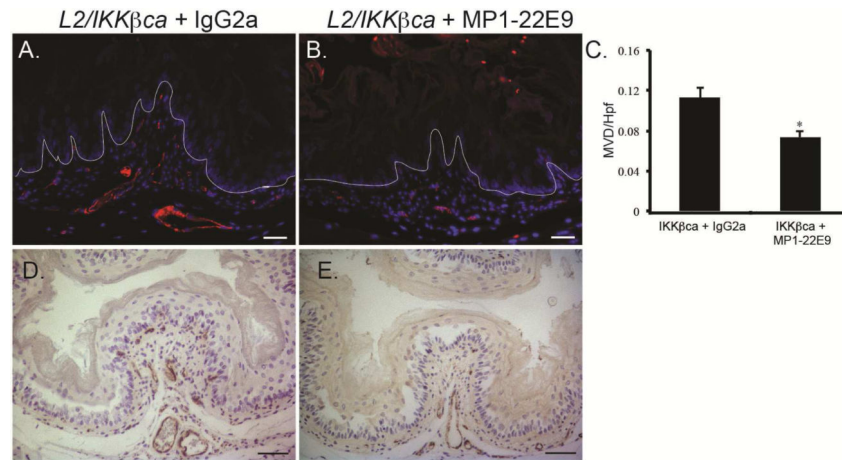


**Figure 6.** GM-CSF inhibition decreases angiogenesis in *L2/IKKβca* mice. (A-E) 4 week-old *L2/IKKβca* mice and their littermate controls were treated with IgG2a control antibody or MP1-22E9 every Monday and Thursday for 2 weeks. (A-B) By immunofluorescence, CD31 positive blood vessels were decreased in *L2/IKKβca* mice treated with MP1-22E9 (B) compared to those treated with IgG2a (A). (n=3 mice per group) (C) Quantification of microvessel density per high power field (MVD/hpf) in mice treated with MP1-22E9 or IgG2a. \*Significant difference from *L2/IKKβca* mice treated with IgG2a at p-value of less than 0.01, Student *t* test. (D-E) Immunohistochemistry revealed decreased numbers of VWF positive endothelial cells in *L2/IKKβca* mice treated with MP1-22E9 (E), compared to those treated with IgG2a (D). (n=3 mice per group) Scale bars, 25 μm (A-B), 50 μm (D-E).

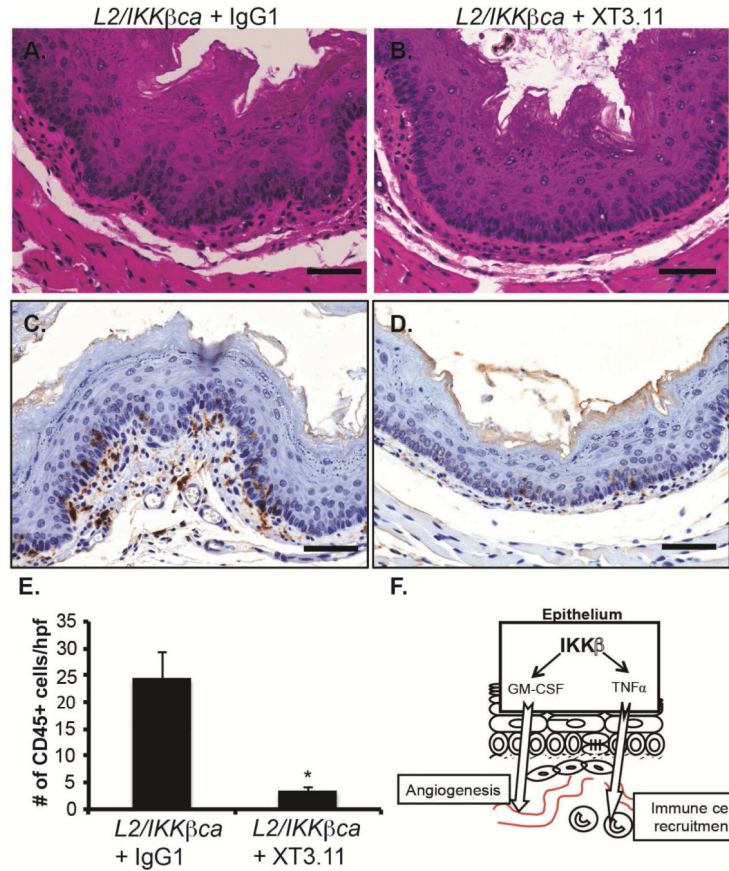


**Figure 7.**

TNF neutralization decreases immune infiltration and inflammation in *L2/IKKβca* mice. (A-D) 4 week-old *L2/IKKβca* mice and their littermate controls were treated with IgG1 control or XT3.11 every Monday and Thursday for 2 weeks. (A-B) Esophageal epithelia of *L2/IKKβca* mice treated with XT3.11 (B) had homogeneous basal cells and regular basal layers compared to *L2/IKKβca* mice treated with IgG1 control antibody (A). (n=4 mice per group) (C-D) By immunohistochemistry, CD45 positive leukocytes were decreased in *L2/IKKβca* mice treated with XT3.11 (D) compared to IgG1 control antibody (C). Scale bars: 50μm. (E) Quantification of the number of CD45 positive cells per high power field (# of CD45+ cells/hpf) in the esophageal mucosa of mice treated with IgG1 control or XT3.11. (n=4 mice per group) \*Significant difference from *L2/IKKβca* mice treated with IgG1 control at p value of less than 0.01, Student *t* test. (F) A model for the role of epithelial IKKβ signaling in inflammation and angiogenesis within the esophagus.